

MODELLING OF CERAMIC TILE SINTERING BY THE SOVS MODEL

J. Balaguer; J.M. Tiscar; A. Saburit; F. Quereda; M. Aguilera

**Instituto de Tecnología Cerámica (ITC). Asociación de Investigación de las
Industrias Cerámicas (AICE)**

Universitat Jaume I. Castellón. Spain.

ABSTRACT

Sintering is a key step in the ceramic tile manufacturing process. In the firing stage, the tile is subjected to a thermal treatment that strengthens and densifies its structure, providing the product with its final aesthetic and physical properties. The sintering process is, therefore, a mass transport process that is activated at high temperature (1/2 or 2/3 of the melting temperature), strengthening interparticle bonds and changing tile porosity and geometry, which is accompanied by a reduction in its free energy. In addition, in the case of vitrified products, the process develops with the

appearance of liquid phase, owing to melting of certain fluxing raw materials in the composition.

Tile softening during sintering can cause the tile to deform under its own weight, affecting both tile dimensional stability and mechanical properties. This phenomenon is known as pyroplasticity, it being particularly critical in low-porosity products, such as porcelain tile, owing to the large amount of liquid phase generated during tile sintering. In industrial practice, this type of product often exhibits problems relating to lack of dimensional stability, curvature, and difficulties in tile cutting. These problems are closely related to the high pyroplasticity and linear shrinkage of such materials, as well as to unequal cooling between the two faces of the tile after sintering, which generates residual stresses in the tile.

To better understand these problems, mathematical models have been developed in recent years to predict tile pyroplastic deformation during firing and the appearance of curvatures and residual stresses in the tile during cooling. However, these models are limited to the bidimensional case and do not take into consideration the densification process. This study was undertaken to extend the mathematical models that describe ceramic tile behaviour during firing, considering the three-dimensional case, together with the densification undergone by the material. To do so, the Skorohod–Olevsky Viscous Sintering (SOVS) model was used to reproduce the firing process of different ceramic materials. The representation of the constitutive model consists of a thermally activated viscous strain, which also depends on the local densification state of the material. To study the tile sintering process, the model was integrated into a finite element simulation software called Salome-Meca.

By laboratory tests and use of the proposed model, the thermal properties of a porcelain tile and energy exchange associated with the chemical reactions that developed during firing were determined. The dependence of tile viscous strain on temperature was then determined. The results of the model show the need to develop a new viscous law that enables sintering kinetics to be adequately predicted.

1. INTRODUCTION

The tile manufacturing process unfolds in a series of successive stages, which can be broken down into three large groups: raw materials preparation, tile forming, and thermal treatment. Thermal treatment, which entails tile sintering, is a key tile manufacturing step, because on it depend most ceramic tile characteristics: mechanical strength, dimensional stability, resistance to chemical agents, cleanability, etc. [1] Moreover, during porcelain tile manufacture, this treatment is particularly liable to cause problems relating to dimensional stability, curvatures, and tile cutting, stemming from the pyroplasticity and high shrinkage of this material during sintering [1], which intensify in the manufacture of large-sized porcelain tile and/or with the presence of pronounced reliefs.

Generally speaking, porcelain tile sintering begins when tile temperature is $1/2$ or $2/3$ higher than body melting temperature, this being high enough to cause significant diffusion and viscous flow in the presence of a large amount of liquid phase. This process reduces tile size and porosity and develops mostly during tile residence time at peak firing temperature. Sintering is, in short, a tile densification process.

The ceramic tile sintering process has been studied by different researchers, who have derived descriptive equations of the sintering kinetics of glaze [2-3] and engobes

[4]. In regard to tile bodies, Orts et al. [5] developed a sintering kinetic model based on isothermal tests. However, no studies were found on the use of constituent equations that describe the physico-chemical development of tiles during sintering. Thus, though there have been recent advances in modelling tile thermo-mechanical behaviour during cooling [6-7], the sintering process has been neglected.

In other fields, however, such as those relating to advanced ceramics, sintering models are widely used to optimise and improve thermal treatment in order to make ceramic tiles with high mechanical properties. One of the models most commonly used in modelling the change in porosity of advanced ceramics during the sintering step is the Skorohod–Olevsky Viscous Sintering (SOVS) model [8], which has been successfully used by several researchers. Argüello et al. [9] used this model to predict ZnO densification. Later, Reiterer et al. [10] correctly predicted the same compound's densification starting from different forming conditions. On the other hand, using the SOVS model, Molla et al. [11] predicted the densification of a solid oxide fuel cell.

The advantage of using constituent equations that describe the sintering process is that, together with the laws of conservation of mass, energy, and linear and angular momentum, the response of a material during the sintering process can be fully described. This is achieved by solving the set of constitutive and conservation equations by numerical methods, such as the finite element method (FEM) [3]. Figure 1 shows the simulation of ceramic tile sintering using the FEM.

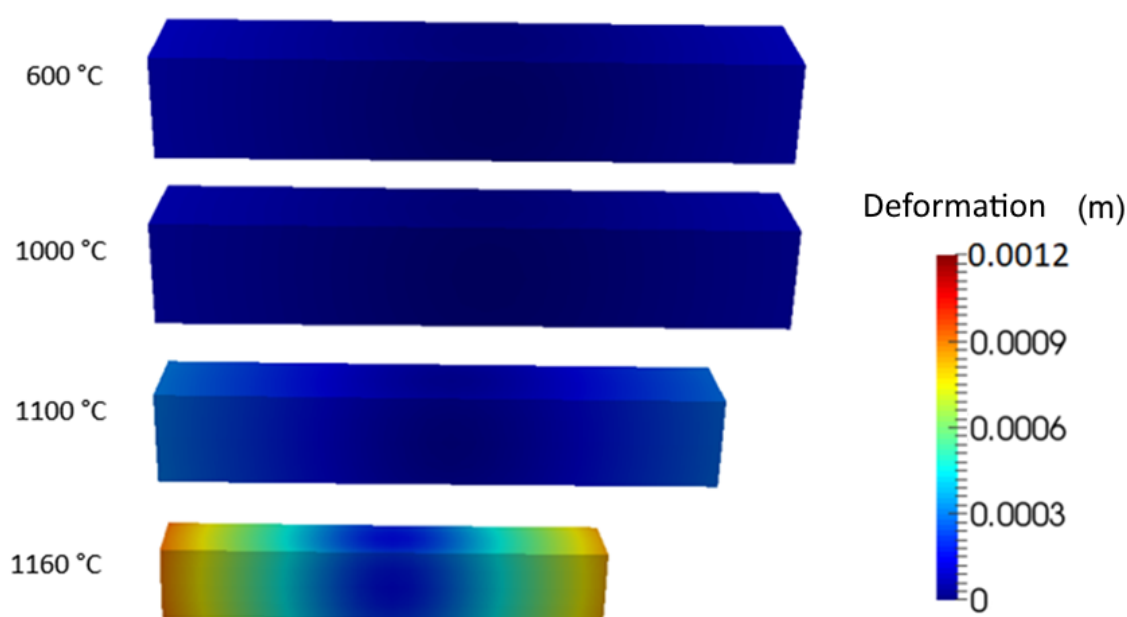


Figure 1. Example of ceramic tile sintering by the FEM.

This study was undertaken to model macroscopically the thermal treatment of ceramic tile bodies in order to optimise process kinetics and improve tile technical properties. The model developed also lays the basis for the study of the behaviour of large-sized ceramic tiles (slabs) and/or with pronounced reliefs, whose thermal treatment requires greater control.

2. THERMO-MECHANICAL MODEL

The constituent model used in this work was the Skorohod–Olevsky Viscous Sintering (SOVS) model [8]. This model incorporates the sintering process as a linear dependent (inelastic) viscous constituent component, among other variables, of temperature:

$$\dot{\epsilon}_{ij}^{in} = \frac{\sigma'_{ij}}{2\eta_0\phi} + \frac{\sigma_{kk} - 3\sigma_s}{18\eta_0\psi} \delta_{ij} \quad (1)$$

$$\frac{\dot{\rho}_r}{\rho_r} = -\dot{\epsilon}_{kk}^{in} \quad (2)$$

Where $\dot{\epsilon}_{ij}^{in}$ represents the inelastic shear strain tensor, σ'_{ij} is the shifting component of the stress tensor, σ_{kk} is the stress tensor trace, σ_s is sintering effective stress, ϕ and ψ represent normalised shear viscosity and normalised volumetric viscosity of the material, which depend on relative density (ρ_r), η_0 is the viscosity of the solid, and δ_{ij} is the Kronecker delta. Finally, $\dot{\rho}_r$ is the variation rate of ρ_r , while $-\dot{\epsilon}_{kk}^{in}$ is the trace of the inelastic shear strain tensor.

The relationship of ϕ , ψ , and σ_s with relative density can be derived from continuous media mechanics [8], so that:

$$\phi = \rho_r^2 \quad (3)$$

$$\psi = \frac{2\rho_r^2}{3(1-\rho_r)} \quad (4)$$

$$\sigma_s = \rho_r^2 \quad (5)$$

The viscosity of the solid is assumed, in a first approximation, to follow the form of an equation of the Arrhenius type:

$$\eta_0 = Ae^{(B/RT)} \quad (6)$$

Where A is a parameter that groups all the diffusion, grain growth and, in general, all those mechanisms involved in the physical rearrangement of the matrix during sintering, B is the process activation energy, R the universal constant of ideal gases, and T temperature. At this point, it may be noted that the form of the viscosity equation is critical to correctly predicting densification development.

As sintering depends on temperature, together with the mechanical description of sintering, it was necessary to introduce the thermal behaviour of the material being studied. Thus, assuming the tile to be an isotropic material with constant thermal conductivity, the equation of heat transmission in a non-steady state and with the presence of chemical reactions adopted the form:

$$\dot{T} = \alpha * \nabla^2 T \quad (7)$$

Where \dot{T} is the rate at which temperature changes and $\alpha *$ is the apparent thermal diffusivity of the material, which depends on temperature and on the N_R chemical reactions that take place during the heat transmission process [12], this being described as:

$$\alpha^* = \frac{\alpha}{1 + \frac{6}{c_p} \sum_{i=1}^{N_R} \frac{\phi_i H_i^0}{T_i^* - T_{*i}} \langle \theta_i \cdot (1 - \theta_i) \rangle} \quad (8)$$

Where α is the real thermal diffusivity of the material; ϕ_i is the fraction of the reference component that takes part in reaction i ; H_i^0 is the enthalpy of reaction i ; T_i^* and T_{*i} are the final and initial temperatures of reaction i ; θ_i is defined as $\frac{T - T_{*i}}{T_i^* - T_{*i}}$, and the symbols $\langle \ \rangle$ represent the Macaulay brackets.

The resolution of the described thermo-mechanical model requires use of numerical methods. In this study, the FEM was used through the Salome-Meca software, incorporating the constitutive model using the MFront code generation tool.

3. EXPERIMENTAL PROCEDURE

3.1. MATERIALS

A typical spray-dried powder porcelain tile composition was used in this study. This composition was chosen to model sintering because of its great shrinkage during firing and, therefore, its greater likelihood to generate sintering defects (calibres, pyroplastic deformation, etc.). The main characteristics of the selected composition are set out below:

Composition	Fired colour	Firing temperature (°C)	Fired bulk density (kg/m ³)
Porcelain tile	White	1160	2400

Table 1. Characteristics of the composition used.

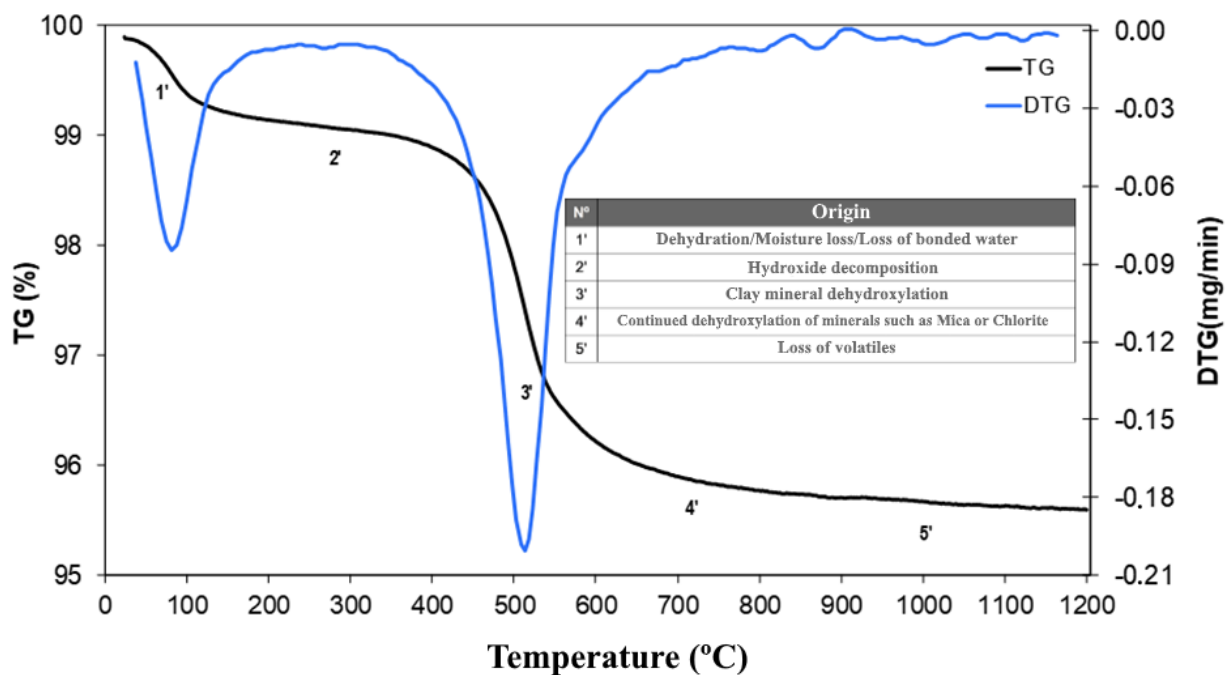


Figure 2. Thermogravimetric (TG) and differential thermogravimetric (DTG) analysis of the composition used.

Porcelain tile test samples were prepared at three different bulk densities for each of the experimental tests. This enabled evaluation of the impact of starting bulk density on sintering kinetics and on the resulting final shrinkage.

3.2. DETERMINATION OF THE THERMAL PARAMETERS

The thermal parameters (Equation 8) were determined by firing test samples of different initial porosity according to different thermal cycles. Initially six cylindrical test samples, 75mm in diameter and 22 mm thick, were prepared. After pressing, holes were drilled in the test samples to set inside a K-type thermocouple, connected to a data logging system recording once a second. The test samples were then dried in an oven at 110°C for 24 hours.

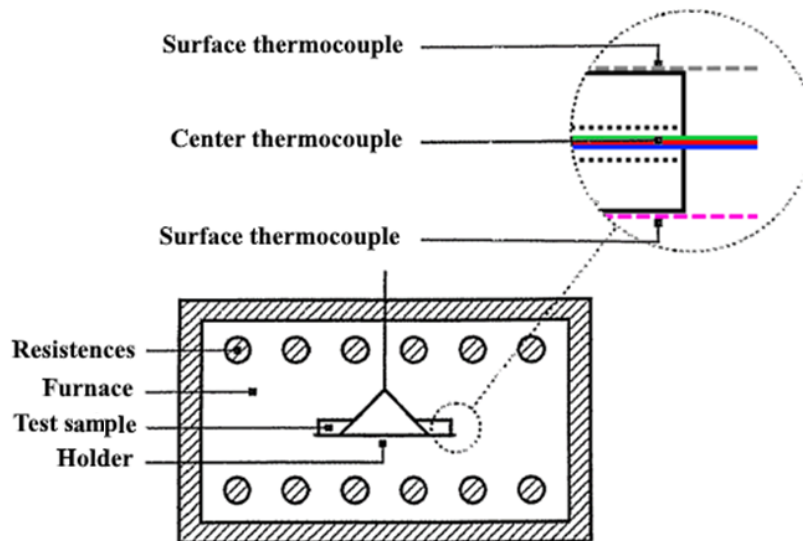


Figure 3. Experimental set-up for determining the thermal parameters. Source: [12].

3.3. MONITORING OF SINTERING BY DILATOMETRY

Porcelain tile densification, starting with the three different bulk densities, was recorded using a contact dilatometer. When the dilatometer furnace was heated, the sample and other furnace components expanded. Recording this expansion by a linear transformer and correcting the expansion corresponding to the furnace components enabled sample expansion to be determined. At high temperature the test samples exhibited high shrinkage owing to the sintering process. In this study, the dilatometer heating rate was 5°C/min to a peak temperature of 1160°C.

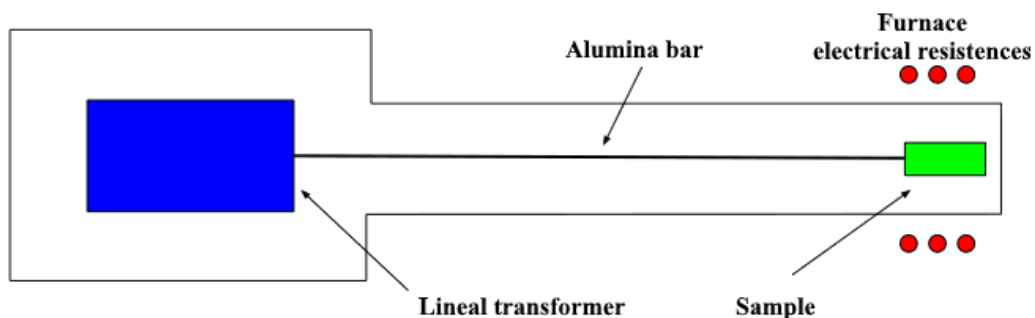


Figure 4. Scheme of a dilatometer.

4. RESULTS

4.1. CALCULATION OF THERMAL PARAMETERS

The test samples prepared according to Section 3.2 were subjected to two thermal treatments with a peak temperature of 700°C and 1100°C, respectively. Test samples heating rate and residence time at peak temperature were 30°C/min and 30 min, respectively, in both cases. Table 2 shows test samples green bulk density and the peak temperature the samples were subjected to during the firing cycle.

Reference	Bulk density, ρ_{ap} (kg/m ³)	Peak firing temperature (°C)
D1-700	1836	700
D2-700	1937	700
D3-700	2052	700
D1-1100	1824	1100
D2-1100	1937	1100
D3-1100	2051	1100

Table 2. Test sample bulk density during determination of the thermal parameters.

The evolution of test samples temperature in different areas according to the thermal cycle to which the samples were subjected is plotted in Figures 5 and 6. The two figures show that, in the studied range, thermal diffusivity (without chemical reaction) hardly changed with test sample bulk density. However, between 550 and 650°C the trend in the temperature evolution changed, which did depend on test sample bulk density. This change in temperature development was related to the presence of a chemical reaction, in this case, of aluminosilicate dehydroxylation (Figure 2).

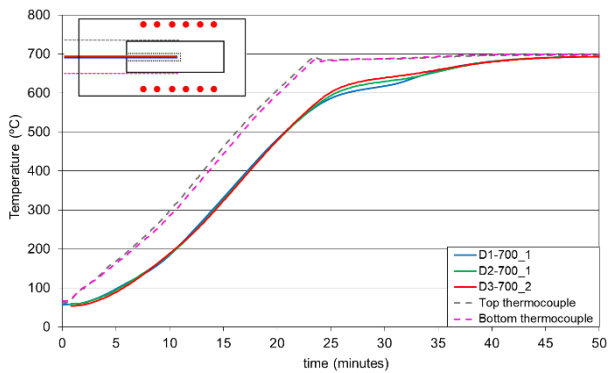


Figure 6. Experimental temperature values obtained on heating the test sample at 700 °C.

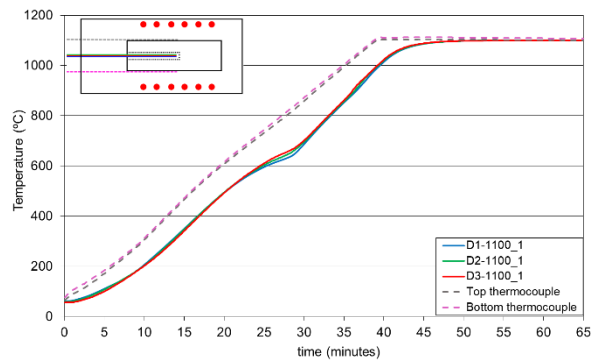


Figure 5. Test sample temperature during firing at 1100 °C.

The same experiments were simulated using the thermal model set out in Section 2 and the Salome-Mecca finite element software multivariate. The thermal parameters were calculated by the Nelder-Mead optimisation method, using the difference between test sample theoretical and experimental centre temperature in both thermal cycles as the target function to be minimised. Thermal diffusivity was determined by applying the optimisation method in a range of temperatures between 25 and 500 °C. On the other hand, the thermal parameters of the dehydroxylation chemical reaction were obtained with the same optimisation method using, in the target function, the experimental results obtained in the temperature range between 500 and 800 °C. Table 3 details the thermal parameters optimised according to this methodology.

Reference	$\bar{\rho}_{ap}$ (kg/m ³)	α (m ² /s)	$\phi_1 H_1^0$ (MJ)	T_1^* (°C)	T_{*1} (°C)
D1	1830	2.64E-07	8.94	882	513
D2	1937	2.46E-07	7.65	871	545
D3	2050	2.35E-07	4.31	783	625

Table 3. Optimised thermal parameters of the studied composition.

In every case, the calorific capacity (C_p) of the test samples was assumed to be constant and equal to 1250 J/(kg·K) [12]. As a result, average thermal conductivity (k) of the test samples, after optimisation, was 0.6 W/(K·m). Test sample theoretical and experimental centre temperature in a firing cycle with a peak temperature of 1100 °C, heating rate of 30 °C/min, and 30 min residence time at peak temperature, is shown in Figure 7. The results show good behaviour of the thermal model with the optimised parameters.

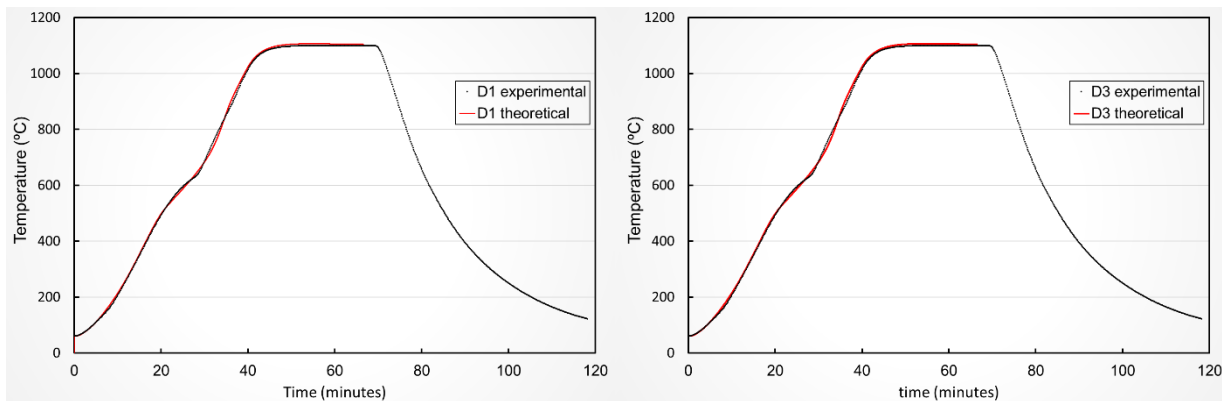


Figure 7. Comparison between the thermal results of the model and the experimentation with test samples D1 and D3, at a peak temperature cycle of 1100°C.

4.2. CALCULATION OF THE SINTERING PARAMETERS

The sintering kinetics were obtained according to the test set out in Section 3.3, whose results are shown in Figure 8A. The difference between the three test samples with different bulk density was significant in the region near 1160°C, where the test sample with the lowest bulk density underwent greater shrinkage than that of the highest density. Note that during heating (25–1000°C), the differences in thermal expansion between the test samples with different bulk densities were negligible.

In the SOVS model used in this study, the sintering fitting parameters were those that defined the evolution of viscosity of the solid with temperature (Equation 6). Using the same procedure as in the calculation of the thermal parameters, an optimisation process was performed by the Nelder-Mead multivariate algorithm, where the target function to be minimised for each test sample was the difference in experimental and simulated expansion, in the temperature range between 900 and 1160°C. Table 4 details the optimised sintering parameters, while Figure 8B depicts a comparison between the experimental and the theoretical sintering results. Note that parameter B was independent of the initial bulk density of the solid as an activation energy was involved, so that the optimum value was common to the three studied test samples.

Reference	ρ_{ap} (kg/m ³)	α (m ² /s)	A (Pa·s)	B (kJ/mol)
D1	1820	2.65E-07	2.59E-4	5.11
D2	1950	2.44E-07	1.99E-4	5.11
D3	2040	2.36E-07	1.63E-4	5.11

Table 4. Optimised sintering parameters.

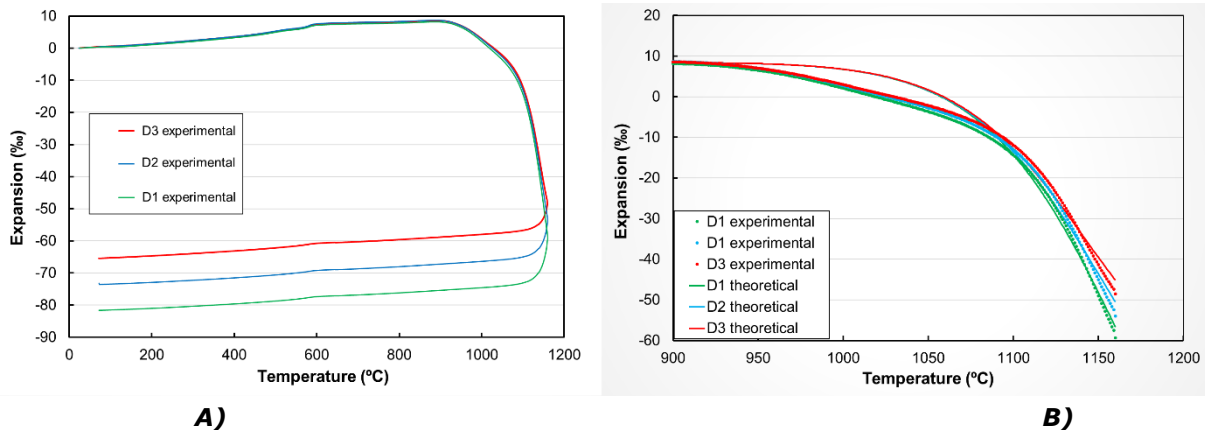


Figure 8. A) Sintering of three test samples with different initial bulk densities. B) Comparison between experimental and theoretical sintering according to the SOVS model after optimisation.

The optimisation results show that the model was unable to predict sintering kinetics in the range of temperatures between 950 and 1100°C, where porcelain tile initial densification took place. Indeed, from 950°C on, the increase in temperature raised the amount of liquid phase and reduced liquid phase viscosity. However, during this first sintering step, mullite crystallisation and quartz dissolution also took place in the composition [13], causing the process to slow down. Finally, from 1100°C on, the sintering rate increased notably, indicating the existence of two clearly differentiated sintering steps [14].

5. CONCLUSIONS

The SOVS model of ceramic tile sintering was implemented in a finite element software to predict tile end characteristics (porosity, shape, etc.) from initial tile geometry, thermal and mechanical properties, and the thermal cycle used. After parameterising the model variables, the results allowed the following conclusions to be drawn:

- The effective thermal diffusivity of a porcelain tile composition formed at different bulk density was characterised. The thermal development predicted by the model during the firing cycle accurately reproduced the experimental values, except during the dehydroxylation reaction, where there were differences, ascribed to the simplifications adopted in modelling effective thermal diffusivity.
- The mechanical model (SOVS) used proved to be able to predict, with relative accuracy, the second sintering step, particularly near peak sintering temperature.
- It was observed that the Arrhenius-type equation chosen to model composition viscosity during sintering did not allow the process to be correctly explained in the range of temperatures between 950 and 1100°C. This could be due to the constant change in the composition of the liquid phase generated during this sintering step. Although liquid phase sintering during the first step was mainly made up of feldspars, mullite crystallisation and quartz dissolution slowed down the sintering process and progressively changed the composition of the stage up to 1100°C. This phenomenon significantly changed the kinetics and evolution of the process, which could not be explained with the proposed model.

Future work will require developing a new viscous law that allows the prediction of sintering kinetics to be improved in the range of temperatures between 900 and 1100°C. This could be done by using two additive viscous laws in order to explain sintering slowdown in this temperature range. In addition, the evolution of tile mechanical properties requires further study. The final results of the model also require laboratory-scale validation, in which theoretical and experimental results can be compared, in addition to validation with large-sized ceramic tiles and complex geometric shapes.

6. REFERENCES

- [1] J. L. Amorós, V. Beltrán, A. Blasco, J. E. Enrique, and A. Escardino, *Defectos de fabricación de pavimentos y revestimientos cerámicos*. Valencia, 1991.
- [2] J. L. Amorós, E. Blasco, A. Moreno, M. P. Gómez-Tena, and C. Feliu, "Non-isothermal sinter-crystallisation of satin glazes: A kinetic model," *Ceram. Int.*, 2018.
- [3] J. L. Amorós, E. Blasco, A. Moreno, and M. P. Gómez-Tena, "Sintering of raw glazes for floor and porcelain tiles: A non-isothermal kinetic model," *Ceram. Int.*, 2016.
- [4] M. Dal Bó, A. O. Boschi, and D. Hotza, "Cinética de sinterización y transporte de masa en engobes cerámicos," *Bol. la Soc. Esp. Ceram. y Vidr.*, vol. 52, no. 5, pp. 237–241, 2013.
- [5] M. J. Orts, J. L. Amorós, A. Escardino, A. Gozalbo, and C. Feliu, "Kinetic model for the isothermal sintering of low porosity floor tiles," *Appl. Clay Sci.*, vol. 8, no. 2–3, pp. 231–245, 1993.
- [6] M. Dal Bó, V. Cantavella Soler, E. J. Sánchez Vilches, D. Hotza, and A. O. Boschi, "Modelización mecánica del enfriamiento rápido en sistemas tipo gres porcelánico," 2012.
- [7] M. Milani, L. Montorsi, M. Venturelli, J. M. Tiscar, and J. García-Ten, "A numerical approach for the combined analysis of the dynamic thermal behaviour of an entire ceramic roller kiln and the stress formation in the tiles," *Energy*, 2019.
- [8] E. A. Olevsky, "Theory of sintering: From discrete to continuum," *Mater. Sci. Eng. R Reports*, 1998.
- [9] J. G. Argüello, V. Tikane, T. J. Garino, and M. V. Braginsky, "Three-dimensional simulation of sintering using a continuum modeling approach," *Proc. Sinter. 2003*, 2003.
- [10] M. Reiterer, K. Ewsuk, and J. Arguello, "An Arrhenius-Type Function to Model Sintering Using the Skorohod-Olevsky Viscous Sintering Model Within a Finite-Element Code," *J. Am. Ceram. Soc.*, vol. 89, pp. 1930–1935, 2006.
- [11] T. T. Molla et al., "Finite element modeling of camber evolution during sintering of bilayer structures," *J. Am. Ceram. Soc.*, vol. 97, no. 9, pp. 2965–2972, 2014.
- [12] V. Cantavella, "Simulación de la deformación de baldosas cerámicas durante la cocción," *Universitat Jaume I*, 1998.
- [13] A. Escardino Benlloch, J. Amorós Albaro, and J. Enrique Navarro, "Estudio de pastas de gres para pavimentos," *Bol. la Soc. Española Cerámica y Vidr.*, vol. 20, no. 1, pp. 17–24, 1981.
- [14] W. D. Kingery, "Introduction to ceramics," 1976.

7. ACKNOWLEDGEMENTS

Project supported by Generalitat Valenciana, through the Valencian Institute for Business Competitiveness (IVACE).